Applied Physics A manuscript No.
(will be inserted by the editor)

Femtosecond dynamics of chemical reactions at surfaces

Ch. Hess, S. Funk, M. Bonn*, D. N. Denzler, M. Wolf and G. Ertl

Fritz-Haber-Institut der Max-Planck-Gesellschaft, Faradayweg 4–6, 14195 Berlin, Germany.

Received: date / Revised version: date

Abstract One of the major goals in physical chemistry is to obtain a microscopic understanding of chemical reactions. Recent developments in femtosecond laser techniques provide the opportunity to resolve the timescale of elementary steps of chemical reactions at surfaces. This is exemplified for the femtosecond laser-induced oxidation of CO on Ru(001). Among other adsorbate-specific probes vibrational sum-frequency generation spectroscopy offers the possibility to monitor adsorbates or reaction intermediates directly at the surface. Recently, we have employed this technique to investigate the dynamics of the CO-stretch vibration of CO adsorbed on Ru(001) after optical excitation leading to CO desorption.

PACS: 68.35.Ja; 78.47.+p; 82.65.-i

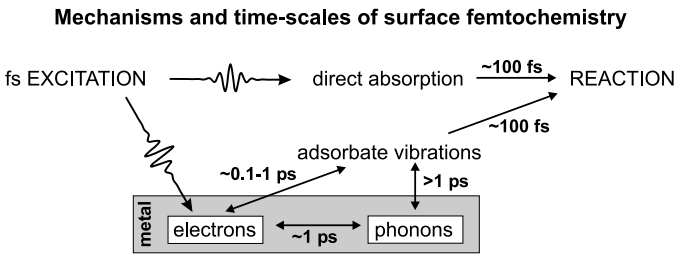

Fig. 1 Diagram of energy flow at metal surfaces after excitation with fs-laser pulses. The timescales of energy exchange between the various subsystems are discussed in the text. Femtosecond-laser radiation excites the substrate electronic system which equilibrates with the lattice phonons within a few ps. Surface reactions can be driven either by an electronic mechanism or by lattice phonons. **FIGURE 1: TWO COLUMNS**

1 Introduction

The dynamics of elementary surface processes like charge and energy transfer and reactions of molecules is of central importance for a microscopic understanding of chemical reactions at solid surfaces e.g. in catalysis [1,2]. Information about these processes can be obtained by initiating the breaking and formation of chemical bonds with femtosecond (fs) laser pulses, probing reaction intermediates at the surface and recording the yield of desorbing reaction products with a mass spectrometer. There are three main issues in surface femtochemistry (among others being related to these): (1) To understand the interaction of photoexcited hot substrate electrons with the adsorbate degrees of freedom. (2) To directly resolve the elementary steps during a surface reaction in order to obtain a mechanistic understanding on a microscopic level. (3) To exploit the different mechanisms and timescales of energy transfer between the substrate and the adsorbate in order to control the outcome of reactions and to open new reaction pathways.

The experimental approach to address these questions is dictated by the timescale of bond breaking. A typical period of an adsorbate-substrate vibration is of the order of 100 fs. Assuming desorption to occur within half a period leads to a timescale of about 50 fs for the simplest surface reaction. In general (as in the case of the CO oxidation) several nuclear rearrangement processes are necessary to achieve a chemical transformation which increases the time for the formation of the reaction products. We use ultrashort laser pulses to achieve the time-resolution necessary to study these processes directly and employ a sequence of two ultrafast laser pulses to initiate and probe the reaction [3].

Figure 1 shows the mechanisms and timescales of surface femtochemistry at metal surfaces. When a fs-laser pulse is absorbed in a metal a hot electron distribution is created within the optical penetration depth (typically 10–100 Å for $h\nu < 10$ eV). These hot electrons may induce chemical reactions at the surface via charge transfer to the adsorbate. Compared to this indirect substrate

* *Present address:* Leiden Institute of Chemistry, P.O. Box 9502, 2300 RA Leiden, The Netherlands.
Correspondence to: wolf_m@fhi-berlin.mpg.de

mediated process direct absorption of light by the adsorbate is orders of magnitude weaker due to the low absorbance of a thin layer of adsorbed molecules (typically a monolayer). As illustrated in figure 1 there are different pathways on which energy can be transferred to the adsorbate degrees of freedom after excitation of the substrate electronic system with fs-laser pulses: Firstly, on a timescale up to several hundreds of femtoseconds the hot substrate electrons can directly excite the substrate-adsorbate system by resonant attachment of an energetic electron into an unoccupied molecular orbital (LUMO). This results in vibrational excitation of the adsorbate and eventually in a reaction. Secondly, the adsorbate vibrations can be excited on a timescale of >1 ps via lattice phonons which are equilibrated with the hot electrons within a few picoseconds (ps). This second pathway is similar to conventional thermal excitation of the adsorbate (or excitation with laser pulses longer than a few ps), in which excited phonons couple vibrational energy into the reaction coordinates.

As will be described in more detail below, a two-pulse-correlation measurement provides a direct way to distinguish between these two reaction pathways, the electron- and phonon-mediated excitation of the adsorbate. Because energy transfer for these two excitation mechanisms occurs on different timescales, the outcome of a chemical reaction, in which one reaction product is formed via the electronic mechanism and another product by the slow phonon-mediated process, can be influenced by changing the temporal width of the laser pulses. Depending on the reaction under investigation, this approach should allow to control the outcome of a chemical reaction at least to a certain degree. However, it should be noted that in the case of substrate-mediated excitation coherence is lost by rapid e–e scattering events and thus application of laser pulses with a specific shaped phase does not provide a further degree of control. This paper reviews the main results for the femtosecond laser induced CO_2 formation on Ru(001) and presents new aspects of the dynamics of the CO-stretch vibration of CO/Ru(001). For a comprehensive overview of substrate-mediated photochemistry the reader is referred to review articles [1,4–6].

2 Experimental

As illustrated in figure 2, the heart of our experimental apparatus consists of an amplified fs-laser system combined with a UHV chamber. The laser system delivers 800 nm (1.5 eV), 110 fs pulses with a pulse energy of about 4.5 mJ per pulse. The fs-seed pulses are intensified by chirped pulse amplification in a regenerative amplifier (Regen) and a multipass amplification stage (Multipass). An extensive description of the experimental setup can be found in reference [7]. In brief, the experiments dealing with the desorption and oxidation of

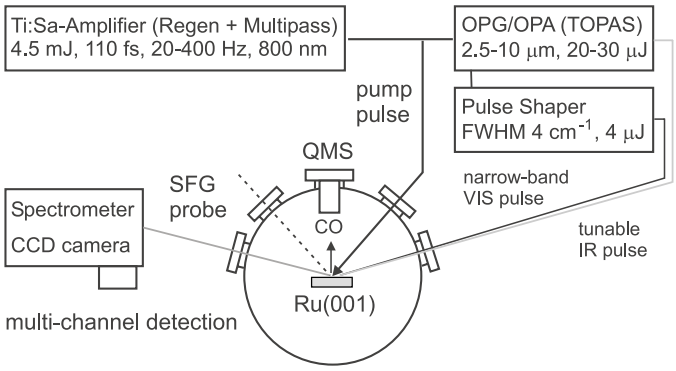

Fig. 2 Schematic diagramm of the experimental setup consisting of an amplified femtosecond laser system and a UHV chamber (see text).

CO were performed directly with the output of the amplifier at 800 nm after reducing the repetition rate to 20 Hz.

The Ru(001) sample was mounted in a UHV chamber (base pressure 1×10^{-10} mbar) and could be cooled to 95 K. The chamber is equipped with a quadrupole mass spectrometer (QMS) and standard surface science tools. Oxygen and CO exposure was performed via a pinhole doser or a variable leak valve. For a detailed description of the surface cleaning, preparation and characterization procedures see reference [7]. In order to prepare the oxygen-precovered surface, 5 L (1 L=1×10^{-6} torr s) of oxygen were dosed onto the sample at 600 K (resulting in an O coverage of 0.5 ML and the formation of the O-(2×1)-structure) followed by CO adsorption at 95 K until saturation.

In a typical experiment we cover the Ru(001) surface with CO and O and measure the reaction yield of desorbing species with the mass spectrometer after fs-laser excitation. Figure 3 shows time-of-flight (TOF) spectra for the desorption of CO and formation of CO_2 after excitation with 800 nm, 110 fs laser pulses. They are obtained by recording the number of molecules coming off the surface as a function of time after fs-laser excitation.

For the sum-frequency-generation (SFG) experiments only part of the output is used to initiate the desorption of CO. The other part pumps an optical parametric amplifier (OPA) with subsequent difference frequency mixing of the signal and idler of the OPA to generate tunable fs-IR pulses (2–10 μm) with a duration of about 150 fs (FWHM) and a pulse energy of 20–30 μJ. SFG is a second-order non-linear optical process in which two incident waves at ω_{VIS} and ω_{IR} generate an output at $\omega_{\mathrm{SFG}}=\omega_{\mathrm{VIS}}+\omega_{\mathrm{IR}}$ where energy and momentum are conserved [9]. The frequency of the IR pulses is chosen to be resonant with the $^{12}C^{16}O$-stretch frequency of CO adsorbed on Ru(001). The residual 800 nm radiation which is not converted in the parametric process is spectrally narrowed to obtain pulses with 4 cm^{-1} bandwidth and is used to upconvert the IR pulses in the SFG experiments. The SFG beam radiated from the

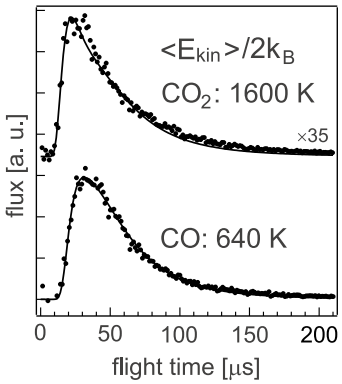

Fig. 3 CO and CO_2 time-of-flight spectra (CO_2 signal multiplied by 35) after fs-laser excitation from CO/O/Ru(001) together with the translational temperatures as a result from the fit (black lines) to the data. The CO_2 data are offset for clarity. Adopted from ref. [8].

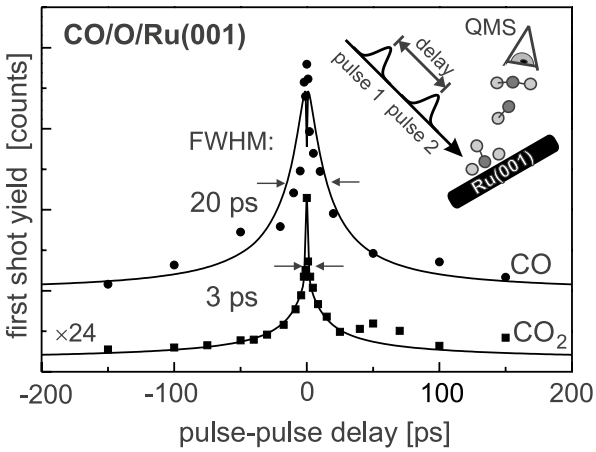

Fig. 4 Two-pulse-correlation measurements for the laser-induced desorption and oxidation of CO indicating the ultrafast response of 3 ps (FWHM) for the CO_2 formation. The lines through the data show the outcome of a friction model calculation using E_a=1.8 eV and τ_{el}=0.5 ps in case of CO_2. The principle of the two-pulse-correlation technique is shown as inset (see text). Adopted from ref. [8].

surface is focused into a spectrograph with a 1200 g/mm grating and dispersed across an intensified CCD detector for multi-channel detection. For the time-resolved SFG experiments a ($\sqrt{3}\times\sqrt{3}$)-CO structure (0.33 ML) of CO/Ru(001) was prepared according to reference [7].

3 Femtosecond laser induced CO_2 formation on Ru(001)

3.1 Results for the femtosecond laser induced reaction between CO_{ad} and O_{ad} on Ru(001)

In the following we summarize the main results for the CO_2 formation and briefly discuss the experimental methods used. Additional information can be obtained from references [7,8]. The oxidation of CO on Ru(001) is a well-described model system [10]. Part of the interest arises from the fact that the Ru(001) surface is the most efficient catalyst for the CO/CO_2 conversion within the group of Platinum metals when working under high pressure oxidizing conditions [11,12]. In contrast, under ultrahigh vacuum conditions Ru(001) is the least active. In particular, under UHV conditions heating of the surface, on which oxygen (0.5 ML) and CO are coadsorbed, does not lead to CO_2 formation at all [13]. Instead, thermal excitation leads to CO desorption between 200–400 K followed by recombinative desorption of oxygen above 1200 K [14]. Because the binding energy of CO/Ru(001) is smaller than the activation energy for O, increasing temperatures lead to ready CO desorption before temperatures are reached at which the O is ready to undergo reaction with CO and therefore no CO_2 formation can take place under these conditions.

However, the CO oxidation reaction can be initiated with strong fs-laser pulses (10–50 mJ/cm^2) [8]. Thus, a new reaction pathway is opened which is not accessible via thermal excitation. This is demonstrated in figure 3 where TOF spectra for CO desorption and oxidation upon fs-laser excitation are shown. The translational temperatures $\langle E_{kin}\rangle/2k_B$ are 640 K for CO and 1600 K for CO_2. The branching ratio between desorption and oxidation is 35±2.5 in favor of desorption. For the CO oxidation to occur the two reactants have to be coadsorbed on the surface (Langmuir-Hinshelwood mechanism). The much higher translational temperature for CO_2 (compared to that for CO) gives a first hint on the dynamics of the process. Obviously, due to energy conservation the higher kinetic energy of the CO_2 molecules is the result of substantial energy release during the CO_2 formation process which is controlled by the shape of the potential energy surface on which the reaction between CO_{ad} and O_{ad} proceeds.

To distinguish between the different mechanisms by which the energy, which is first deposited in the substrate electronic system, can flow into the adsorbate degrees of freedom, we employ a two-pulse correlation measurement. Figure 4 depicts the result of such measurements for CO and CO_2. As shown schematically in the inset, two 800 nm fs-laser pulses, which are delayed with respect to each other, are sent to the CO/O/Ru(001) surface and the CO/CO_2 yield is recorded as a function of delay time between the pulses. The observation of a correlation signal for CO and CO_2 around zero delay is a consequence of the nonlinear fluence dependence of the CO/CO_2 yield [8]. From the two-pulse-correlation measurement one obtains information on the lifetime of the excitation responsible for the CO_2 formation. When using two laser pulses with an energy of about 1.5 mJ each, the first laser pulse excites the electrons to temperatures of about 2000 K. Subsequently, they cool down

within 1.5 ps due to equilibration with the phonons. For delays within this time period (given by the electron-phonon coupling strength) the second excitation pulse acts to further enhance the temperature of the hot electrons. The two-pulse correlation for CO_2 shows an ultrafast response of 3 ps (FWHM) which correlates with the timescale on which the hot electrons start to equilibrate with the lattice phonons. Thus, we can assume the CO oxidation to be driven by an electronic excitation mechanism. On the other hand, the slow response of 20 ps (FWHM) for the CO desorption implies coupling to phonons. This is corroborated by the fact that a simulation using the friction model [15,16] can reproduce the two-pulse correlation very well with coupling to phonons only. In addition, the relevant molecular resonance (LUMO), at least for CO adsorbed on clean Ru(001), is located at 4.9 eV above the Fermi level [17] which is too high in energy to be efficiently populated by hot electron attachment [7].

Now, we address the question whether the excitation of the adsorbed CO or oxygen determines the CO_2 yield which is crucial for a mechanistic understanding of the reaction. In order to distinguish between these two excitation pathways CO- and oxygen-isotope experiments were performed by covering the surface with a 50/50-mixture of $^{16}O/^{18}O$ or $^{12}C^{16}O/^{13}C^{16}O$ and coadsoption of the other reaction component, respectively. Whereas for CO no isotope effect concerning CO_2 formation is present, one obtains a pronounced isotope effect of 2.2±0.3 for the yield ratio $^{16}OCO/^{18}OCO$. Such an isotope effect is expected for an electronically mediated process (as known from DIET (Desorption induced by electronic transitions) [18]), and therefore confirms the aforementioned assumption of electronically excited oxygen as the primary step in the CO oxidation. The results of the isotope effect measurements indicate that the activation of the Ru-O bond is the rate-determining step in the CO oxidation process. The width of the two-pulse-correlation measurement allows to unravel the nature of the excited oxygen in more detail. A friction model calculation for the CO_2 formation (shown as solid line in figure 4) results in a *finite* coupling time of the adsorbate degress of freedom to the electrons of τ_{el}=0.5 ps [8]. Therefore, we conclude that the oxygen that reacts with CO is *vibrationally* excited in the electronic ground state. In contrast, in a scenario with oxygen reacting from an electronically excited state, we would expect a much smaller coupling time on the order of excited-state lifetimes on metal surfaces of typically 1–10 fs [19].

3.2 Proposed mechanism for the CO_2 formation on Ru(001)

From these findings we deduce the following mechanism for the reaction of CO with coadsorbed oxygen atoms on a Ru(001) surface, as illustrated in figure 5: Upon optical excitation with a strong fs-laser pulse a hot-electron

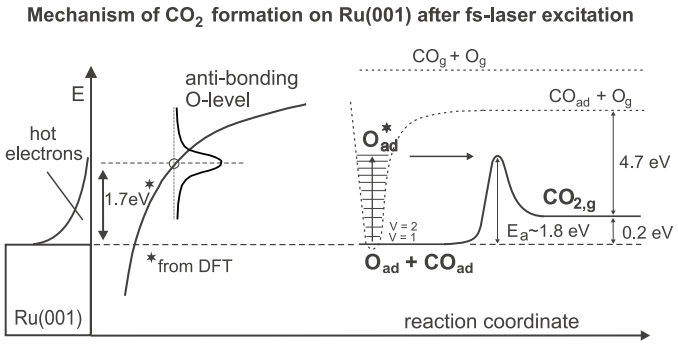

Fig. 5 Mechanism for the CO_2 formation on Ru(001) induced by fs-laser excitation. Starting from the hot electron distribution created with the fs-laser pulse, occupation of an antibonding orbital of the Ru-O-bond leads to a weakening of the bond and subsequent reaction with coadsorbed CO. Note that energies are not in scale. **FIGURE 5: TWO COLUMNS**

distribution, characterized by transient temperatures of the Fermi distribution of about 4000–5000 K, is created within the substrate. At such high temperatures electrons may be resonantly attached to an unoccupied antibonding orbital of the oxygen-Ru bond, which according to density functional theory (DFT) calculations [8], is located at about 1.7 eV above the Fermi level. The transient occupation of this adsorbate resonance leads to energy transfer from the hot electrons to the Ru-O bond via electronic friction [15]. This results in *vibrational* excitation of the Ru-O bond which is ready to undergo reaction with coadsorbed CO. Due to its high binding energy at a coverage of 0.5 ML (about 4.9 eV [20]) no recombinative oxygen desorption after fs-laser excitation is observed. In contrast, the reaction between oxygen and carbon monoxide leads to translational highly excited CO_2 with kinetic energies corresponding to temperatures of about 1600 K as shown in the TOF spectrum in figure 3. Considering the potential energy diagramm for $CO_{ad}+O_{ad}\rightarrow CO_2$ we can understand the origin of this excess in translational energy. Due to the creation of the thermodynamically stable CO_2, expressed by its low Gibbs energy, part of the energy released during the formation of CO_2 is channeled into the translation in addition to energy transfer to the vibrational and rotational modes. From the results of our isotope experiments we conclude that the activation of the strongly bound oxygen is the rate-determining step for the formation of CO_2. Therefore, we can determine the energy barrier for the reaction to be about 1.8 eV by using the electronic friction model to describe the oxygen activation (see figure 4). Recent density functional calculations of the CO oxidation for the Ru(001)-p(2×2)-(CO+O) structure by Alavi et al. [21] determine the reaction barrier to be 1.4 eV. According to this study the crucial step in the CO oxidation is the activation of the strongly bond oxygen atom which is in agreement with our experimental result. From their calculations Alavi

et al. conclude that the O activation results in a movement from a three-fold hollow site to a bridge site on a timescale of about 120 fs. Simultaneous movement of O and CO towards each other is supposed to lead to reaction. Starting from a Ru(001)-(1×1)-O structure with CO coadsorbed in an oxygen vacancy Stampfl and Scheffler calculate the energy barrier for CO_2 formation to be approximately 1.5 eV. The minimum energy path for this process corresponds to essentially direct movement of the CO molecule towards the O atom leading to a transition state in which CO and O have substantially weakened their bond to the substrate [22].

4 Time-resolved femtosecond laser spectroscopy

The techniques described above are all based on the detection of the desorbing reaction products in the gas phase. However, other molecule-specific methods are necessary to follow reactions directly on the surface as they proceed from reactants to products. Due to the recent advances of ultrafast laser sources and especially the development of nonlinear laser-based surface probes various approaches to tackle this problem have become accessible as illustrated in figure 6. Common to all this methods is the pump-probe technique in combination with a molecule or surface specific probe. An intense ultrafast laser pulse (pump pulse) initiates a reaction of adsorbed molecules. The resulting changes in the adsorbate-substrate system are monitored at later times with a second ultrafast laser pulse. While in gas- and liquid-phase chemistry this technique is widely employed [3], the application to ultrafast surface dynamics is still at the beginning. This is due to several reasons: (1) The fact that in surface science typically only a monolayer (or less) of adsorbed molecules is studied leading to a small optical density. (2) The large contribution of the bulk to the signal which requires the use of nonlinear optical techniques. (3) The complexity of energy dissipation and electronic coupling between a solid and an adsorbate which governs the reaction dynamics at solid surfaces.

There are various methods to probe changes in the adsorbate-substrate system after excitation with a pump pulse (figure 6 right). Time-resolved infrared reflection absorption spectroscopy (IRAS) [24] and second harmonic generation (SHG) [9] have been employed to study the energy exchange and desorption dynamics of CO with various transition metal surfaces [25–27]. Recently, two-photon photoemission (2PPE) [28] has been used to elucidate the dynamics of the cesium-copper bond-breaking process by analyzing dynamic changes in the surface electronic structure [29]. Whereas IRAS as a linear optical technique is suffering from a large background contribution, SHG and 2PPE do not have the potential to take adsorbate-specific snapshots during the course of a surface reaction. Therefore, we employ the nonlinear optical technique of infrared-visible sum-frequency

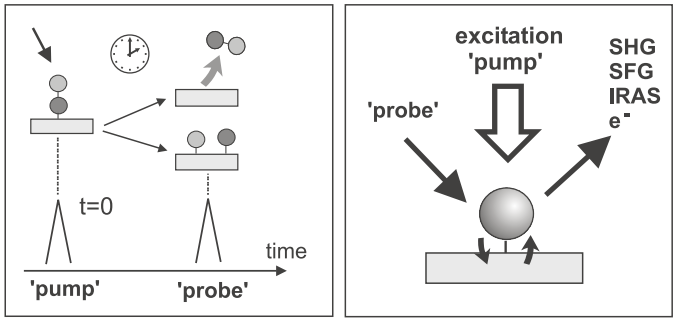

Fig. 6 Methods of time-resolved spectroscopy on surfaces based on the pump-probe technique: An ultrafast laser pulse ('pump') initiates a reaction of adsorbed molecules. Changes in the adsorbate-substrate system are monitored at later times with a second ultrafast laser pulse ('probe').

generation (SFG) due to its surface sensitivity and adsorbate specifity [9,23].

5 Time-resolved SFG spectroscopy

Sum-frequency-generation (SFG) has become a versatile tool for the study of molecules at surfaces [30]. It combines the interface selectivity of second-order nonlinear optical processes with the adsorbate specifity of a spectroscopic technique. In particular, IR-visible SFG can be used to perform surface spectroscopy of vibrational transitions by scanning a laser in the infrared. For our experiments we use fs-IR pulses which inherently provide a broad spectral bandwidth of about 150 cm^{-1} (FWHM). Therefore, the SFG signal at frequencies ω_{IR} that are resonant with the vibrational transition will be resonantly enhanced [31]. This is shown on the lower right of figure 7 which displays a typical SFG spectrum of the CO-stretch vibration of $(\sqrt{3}\times\sqrt{3})$-CO/Ru(001) together with the IR spectrum of the broadband-IR pulses used in the experiment. Such an experimental approach offers the possibility to achieve spectral resolution when employing narrowband-visible pulses and a good time-resolution (limited by the duration of the IR pulse and the pump pulse and the free-induction decay of the vibration (see below)). Typically, a time resolution of about 500 fs and spectral resolution of 8 cm^{-1} is achieved [23]. Recently, the high sensitivity of broadband-IR SFG spectroscopy has been demonstrated by recording vibrational spectra of CO/Ru(001) at coverages as low as 0.001 ML. Besides, the broad spectral range covered by the IR-pulse can be exploited to simultaneously observe the fundamental and hot-band transition of a resonance without tuning the IR frequency [32].

There are basically two types of time-resolved SFG measurements. The first type of experiment can measure the dephasing time T_2 of a vibrational resonance: An infrared pump pulse coherently excites the vibrational polarization which subsequently decays due to dephasing (free induction decay). The remaining coherence is

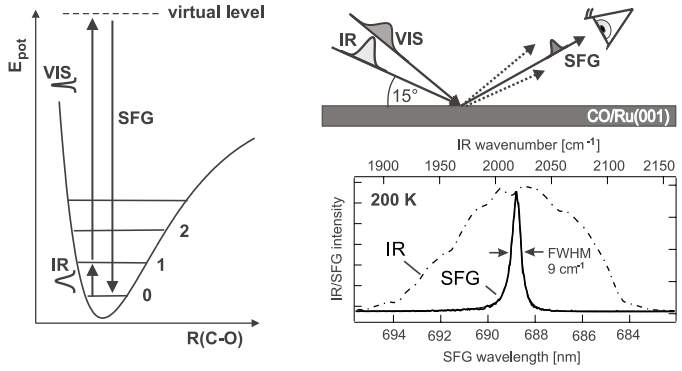

Fig. 7 Left: Principle of IR-VIS-SFG (see text). Right top: Scheme for broadband-SFG. Right bottom: SFG spectrum of the CO stretch vibration of $(\sqrt{3}\times\sqrt{3})$-CO/Ru(001) at 200 K (black line). The spectrum of the broadband-IR pulse is shown as dashed curve. **FIGURE 7: TWO COLUMNS**

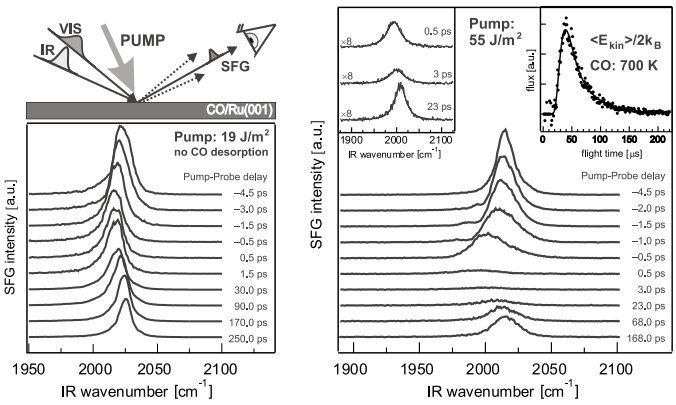

Fig. 8 Transient SFG spectra of the CO-stretch vibration of CO/Ru(001) after excitation with a pump pulse of low fluence (19 J/m^2, left panel) and high fluence (55 J/m^2, right panel). Left top: Scheme for broadband-SFG as probe after excitation with an intense pump pulse. When a pump pulse with a sufficiently high fluence is used desorption of CO is initiated as can be seen from the TOF spectrum shown as inset in the right panel. Part of the figure is adopted from ref. [23] **FIGURE 8: TWO COLUMNS**

probed with the visible upconversion pulse which is delayed with respect to the infrared. From the exponential decay exp(-t/τ) of the SFG intensity the dephasing time T_2=2τ can be obtained [33]. For example, for $(\sqrt{3}\times\sqrt{3})$-CO/Ru(001) at 340 K a dephasing time of T_2=1.2 ps is observed [23]. The second type of experiment employs an intense pump pulse for photo-excitation of the substrate-adsorbate system and a weak SFG probe to monitor the changes induced by the pump pulse.

In the following, an example for the application of the pump-probe technique using near-infrared fs-laser pulses as pump and SFG spectroscopy as probe is given: The CO-stretch vibration of CO adsorbed on Ru(001) is investigated after 800 nm fs-laser excitation [23]. The fluence of the pump pulse is chosen to reveal the changes in the CO-stretch vibration within two distinct excitation regimes: A low fluence regime (shown on the left of figure 8), in which - starting from a colder surface (T_s=95 K) - no desorption of CO occurs, and a high fluence regime (shown on the right of figure 8) in which sufficiently strong excitation - starting from a temperature of T_s=340 K - initiates desorption of CO molecules. This is demonstrated in the inset of figure 8 which depicts the TOF spectrum of the photodesorbed CO molecules. The translational temperature of 700 K is slightly lower than the calculated adsorbate temperature of about 900 K. This translational cooling is consistent with former investigations on the desorption of CO from CO/Ru(001) and is indicative for a phonon-driven desorption process which is too fast in order to achieve accommodation onto the surface [7].

During the laser shots the surface is redosed via the background (p_{CO}=5×10^{-6} mbar) and through thermal diffusion of CO on the surface. The data (figure 8) shown incorporate several interesting features as a transient redshift and a broadening of the CO resonance. These are much more pronounced for the high fluence regime in which, in addition, a strong decrease in the SFG intensity is visible. The fact that the redshift of the resonance starts already at negative delay times is due to the finite lifetime of the IR polarization induced by the IR pulse [34]. Therefore, the pump pulse induces a redshift on the timescale of the decaying vibrational polarization (T_2=1.2 ps). In the following discussion we will focus on the frequency shift of the resonance.

In order to explain the transient redshift several factors that influence the spectral position of the CO-stretch vibration in the experiment have to be taken into account: (1) Increasing temperature leads to a downshift in frequency due to anharmonic coupling of the CO-stretch vibration to the frustrated translational mode [35]. This effect partially explains the transient redshift seen in the experiment. Also, the calculated phonon temperature profile after excitation with a fs-pulse resembles the temporal evolution of the frequency very well [23]. (2) Decreasing CO coverage leads to a downshift in frequency due to reduced dipole-dipole coupling [35]. Since the CO coverage decreases monotonically with time within the experiment, this effect can not account for the transient behavior of the blueshift following the redshift. (3) Due to anharmonic coupling of the CO-stretch vibration to the low-frequency modes of CO/Ru(001) around 500 cm^{-1} (see figure 9) red- and blueshifts of the CO-stretch frequency are possible and will be outlined in the following. Whereas for the low fluence regime the transient shift in frequency can be exclusively explained by anharmonic coupling of the CO-stretch vibration to the frustrated translation (mechanism (1)), the situation is more complex in the high fluence regime.

As all of the lower frequency modes that can couple to the CO-stretch vibration have frequencies in the range of 40–500 cm^{-1} (see figure 9), they can be thermally excited at the high temperatures reached in the

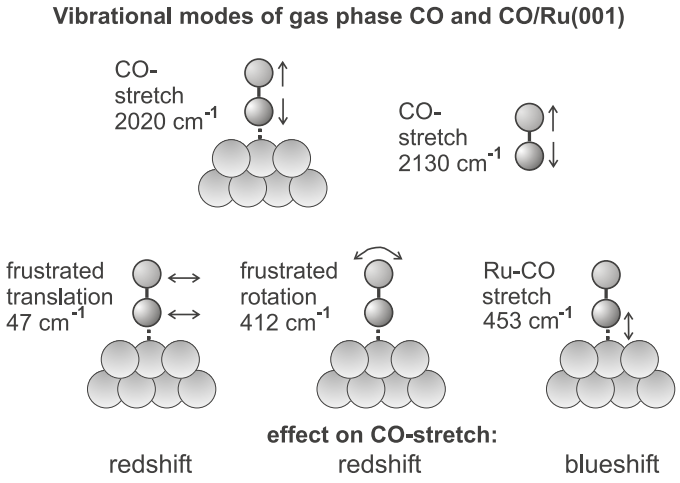

Fig. 9 Vibrational modes of gas phase CO and CO/Ru(001) and their effect on the frequency of the CO-stretch vibration (see text).

desorption experiment. The stretching of the CO-metal bond will lead to a *blueshift* since in the limit of large distances of CO from the surface the CO frequency must approach the gas phase value of 2130 cm^{-1}. Therefore, excitation of this CO-Ru stretch can not explain the experimental data. In case of excitation of the frustrated translation a *redshift* of the CO-stretch frequency is expected as a result of anharmonic coupling to the frustrated translational mode [35]. It arises from a weakening of the CO bond due to displacement of the CO molecule from its top position towards the bridge site. However, calculations show that coupling to the CO translation alone cannot account for the experimental findings [23]. The effect of the rotational mode on the CO-stretch frequency with changing temperature has not been investigated experimentally. From linewidth measurements using IR spectroscopy [36] this mode is found to depend strongly on temperature which might therefore explain the strong increase in linewidth from the low to the high fluence regime. We note that for CO/Cu(100) the frustrated rotational mode is identified to contribute significantly to the desorption of CO [37].

Summarizing, we conclude that the coupling of the internal CO-stretch vibration to the frustrated rotational mode must be crucial to explain the transient redshift, in addition to coupling to the frustrated translation. This is confirmed by analyzing the effect of anharmonic coupling to different modes on the linewidth of the CO resonance. Whereas the coupling to the metal-CO mode is negligible small, efficient coupling to the frustrated translation and especially the frustrated rotation can explain the observed increase in linewidth of about an order of magnitude [23].

6 Conclusions

There is now an emerging understanding of the mechanisms of surface femtochemistry obtained by a variety of experimental methods: Among these are measurements of the translational energy distributions, two-pulse-correlations and isotope effects of desorbing molecules and reaction products after fs-laser excitation. In combination with theoretical investigations an understanding of the mechanisms underlying simple chemical reactions becomes possible now, as demonstrated for the CO oxidation on Ru(001). This study and earlier studies e.g. on O_2 desorption from Pd(111) [38] and Pt(111) [39] lead to the conclusion that electron-mediated surface reactions might be of more general relevance in surface femtochemistry. The use of new fs-laser technology in combination with nonlinear optical spectroscopies allows to investigate surface chemical reactions directly in the time domain. Hereby, the ultimate goal is to resolve individual steps in chemical reactions by identification of short-lived reaction intermediates. Infrared-visible sum-frequency generation spectroscopy as an adsorbate-specific probe seems to be a promising tool to achieve this goal in the near future. This technique has been applied to CO/Ru(001) to study the dynamics of adsorbate vibrations under conditions where desorption is occurring.

7 Acknowledgements

We thank C. Stampfl, M. Scheffler and B. Persson for valuable contributions and J. Miners for experimental help. This work was supported in part by the Deutsche Forschungsgemeinschaft through SFB 450.

References

1. R.R. Cavanagh, D.S. King, J.C. Stephenson and T.F. Heinz, J. Phys. Chem. **97**, 786 (1993)
2. H.-L. Dai and W. Ho, Eds. *Laser Spectroscopy and Photochemistry on Metal Surfaces* (World Scientific, Singapore 1995)
3. A. Zewail, J. Phys. Chem. A **104**, 5660 (2000)
4. E. Hasselbrink, Ber. Bunsenges. Phys. Chem. **12**, 1692 (1993)
5. X.Y. Zhu, Ann. Rev. Phys. Chem. **45**, 113 (1994)
6. W. Ho, Surf. Sci. **299/300**, 996 (1993)
7. S. Funk, M. Bonn, D.N. Denzler, Ch. Hess, M. Wolf and G. Ertl, J. Chem. Phys. **112**, 9888 (2000)
8. M. Bonn, S. Funk, Ch. Hess, D.N. Denzler, C. Stampfl, M. Scheffler, M. Wolf and G. Ertl, Science **285**, 1042 (1999)
9. Y.R. Shen, Nature **337**, 519 (1989)
10. A. Böttcher, H. Niehus, S. Schwegmann, H. Over and G. Ertl, J. Chem. Phys. B **101**, 11185 (1997)
11. C.H.F. Peden and D.W. Goodman, J. Chem. Phys. **90**, 1360 (1986)
12. C.H.F. Peden, D.W. Goodman, M.D. Weisel and F.M. Hoffmann, Surf. Sci. **253**, 44 (1991)

13. K.L. Kostov, H. Rauscher and D. Menzel, Surf. Sci. **278**, 62 (1992)
14. T.E. Madey, H.A. Engelhardt and D. Menzel, Surf. Sci. **48** 304 (1975)
15. M. Brandbyge, P. Hedegård, T.F. Heinz, J.A. Misewich and D.M. Newns, Phys. Rev. B **52**, 6042 (1995)
16. L.M. Struck, L.J. Richter, A. Buntin, R.R. Cavanagh and J.C. Stephenson, Phys. Rev. Lett. **77**, 4576 (1996)
17. C. Benndorf, E. Bertel, V. Dose , W. Jacob, N. Memmel and J. Rogozik, Surf. Sci. **191** 455 (1987)
18. P. Avouris, R.E. Walkup, Ann. Rev. Phys. Chem. **40**, 173 (1989)
19. H. Zacharias, Appl. Phys. A. **47**, 37 (1988)
20. C. Stampfl, S. Schwegmann, H. Over, M. Scheffler and G. Ertl, Phys. Rev. Lett. **77**, 3371 (1996)
21. C. J. Zhang, P. Hu and A. Alavi, J. Chem. Phys. **112**, 10564 (2000)
22. C. Stampfl and M. Scheffler, Surf. Sci. **433**, 119 (1999)
23. M. Bonn, Ch. Hess, S. Funk, J. Miners, B.N.J. Persson, M. Wolf and G. Ertl, Phys. Rev. Lett. **84** 4653 (2000)
24. P. Dumas, M.K. Weldon, Y.J. Chabal and G.P. Williams, Surf. Rev. Lett. **6**, 225 (1999)
25. J.A. Prybyla, H.W.K. Tom and G.D. Aumiller, Phys. Rev. Lett. **68**, 503 (1992)
26. T.A. Germer, J.C. Stephenson, E.J. Heilweil and R.R. Cavanagh, Phys. Rev. Lett. **71**, 3327 (1993)
27. J.P. Culver, M. Li, L.G. Jahn, and R.M. Hochstrasser, Chem. Phys. Lett. **214**, 431 (1993)
28. R. Haight, Surf. Sci. Rep. **21**, 275 (1996)
29. H. Petek, M.J. Weida, H. Nagano and S. Ogawa, Science **288**, 1402 (2000)
30. G.A. Reider and T.F. Heinz, in: *Photonic Probes of Surfaces* Ed. P. Halevi (Elsevier Science, Amsterdam 1995) p. 413
31. L.J. Richter, T.P. Petralli-Mallow and J. C. Stephenson, Opt. Lett. **23**, 1594 (1998)
32. Ch. Hess, M. Bonn, S. Funk and M. Wolf, Chem. Phys. Lett. **325**, 139 (2000)
33. T. Mii and H. Ueba, Surf. Sci. **427–428**, 324 (1999)
34. T.A. Germer, J.C. Stephenson, E.J. Heilweil and R.R. Cavanagh, J. Chem. Phys. **101**, 1704 (1994)
35. P. Jakob and B.N.J. Persson, Phys. Rev. B **56**, 10644 (1997)
36. P. Jakob, J. Chem. Phys. **108**, 5035 (1998)
37. C. Springer, M. Head-Gordon and J.C. Tully, Surf. Sci. **320**, L57 (1994)
38. J.A. Misewich, A. Kalamarides, T.F. Heinz, U. Höfer and M.M.T. Loy, J. Chem. Phys. **100**, 736 (1994)
39. S. Deliwala, R.J. Finlay, J.R. Goldman, T.H. Her, W.D. Mieher and E. Mazur, Chem. Phys. Lett. **242**, 617 (1995)